

SCATTERING AND PICK-UP REACTIONS WITH DEUTERONS ON Be, B, C, N AND O AT 11.8 MeV

W. HITZ, R. JAHIR and R. SANTO

Max-Planck-Institut für Kernphysik, Heidelberg, Germany

Received 24 May 1967

Abstract: The elastic deuteron scattering data from Be, ^{10}B , ^{11}B , C, N and O have been analysed in terms of the optical model. It was possible to obtain optical parameters which show only small variations from one nucleus to the other. Experimental angular distributions of deuterons from the (d, d') reactions on ^9Be , ^{10}B and ^{12}C , of tritons from the (d, t) reactions on ^9Be , ^{10}B and ^{11}B and of ^3He particles from the (d, ^3He) reactions on ^{10}B and ^{11}B have been analysed in terms of the DWBA theory. Satisfactory fits to the pick-up data were obtained using the deuteron potentials derived from the elastic scattering. Spectroscopic factors have been extracted and are compared with intermediate coupling calculations.

F

NUCLEAR REACTIONS ^9Be , ^{10}B , ^{11}B , C, N, O (d, d), (d, d'), (d, t), (d, ^3He),
 $E = 11.8 \text{ MeV}$, measured $\sigma(E_{d'}, \theta)$, $\sigma(E_t, \theta)$
 $^{8, 9, 10}\text{Be}$, $^{10, 11}\text{B}$ deduced levels, spectroscopic factors Enriched $^{10, 11}\text{B}$ targets

1. Introduction

For the analysis of direct nuclear reactions, the DWBA method which is based on the optical model of elastic scattering, is most widely applied. However in the region of very light nuclei, this procedure encounters more difficulties than for heavier nuclei. Recently it has been possible to obtain a reasonable agreement with the deuteron scattering data on carbon within a wide energy range by means of optical-model calculations ⁶⁾.

The aim of the present work was to investigate the elastic deuteron scattering data on light nuclei and to find a common set of parameters for different target nuclei. Further, it was interesting to see if the DWBA method gives a reasonable agreement with experimental data of (d, d'), (d, t) and (d, ^3He) reactions, using optical parameters derived from elastic scattering. In the course of the present investigation we have included some data on elastic and inelastic deuteron scattering ^{1, 2)} and on (d, t) and (d, ^3He) reactions ^{3, 4)}, which have been taken earlier in this laboratory.

2. Experimental procedure

The deflected and analysed deuteron beam of the Heidelberg cyclotron with a total energy spread of about 60 keV was focussed to an area of $3 \times 3 \text{ mm}^2$ on the target in the centre of a 50 cm diam scattering chamber. Different types of particles have been identified by the $dE/dx \cdot E$ technique.

A dE/dx silicon surface-barrier counter of 50 μm thickness has been used for the spectroscopy of deuterons down to an energy of about 3 MeV. Since this counter already absorbed ^3He particles with an energy as high as 8 MeV, it has been replaced in part of the measurements by a proportional counter tube operating at a pressure of 50–200 Torr methane. With this device, spectroscopy of ^3He particles down to 3.3 MeV and of tritons down to 2.2 MeV energy was possible.

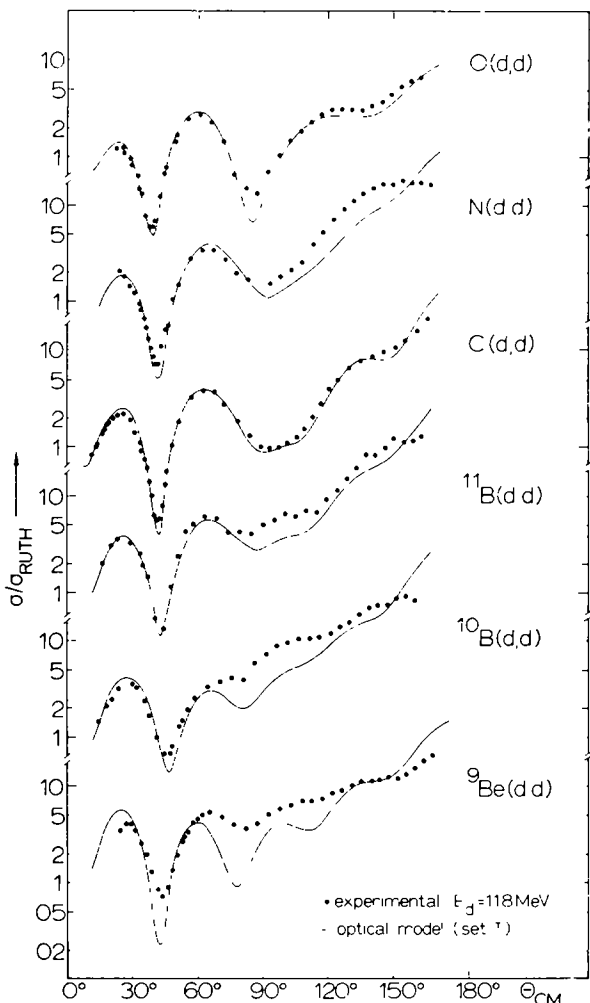


Fig. 1. Experimental angular distributions of the elastic deuteron scattering from Be, ^{10}B , ^{11}B , C, N and O in terms of the Rutherford cross section. The solid curves are the result of calculations with type I optical-model parameters.

The ^{10}B target has been made by evaporation with an electron gun from boron powder enriched to 96.5 % in ^{10}B . The total target thickness was 250 $\mu\text{g}/\text{cm}^2$ (150

$\mu\text{g}/\text{cm}^2$ boron, the other components being carbon, oxygen and a small amount of nitrogen). In the very forward angles, the elastic lines of these components have not been resolved, and the boron cross section has been determined by subtracting the contributions of the contaminations known from the other measurements. The same procedure was necessary in the ^{11}B case, where a target with $20 \mu\text{g}/\text{cm}^2$ ^{11}B was available.

3. Results

At $E_d = 11.8$ MeV, the $^{10}\text{B}(d, d)$ and $^{11}\text{B}(d, d)$ angular distributions have been measured. The previous $\text{Be}(d, d)$, $\text{C}(d, d)$ and $\text{O}(d, d)$ measurements have been

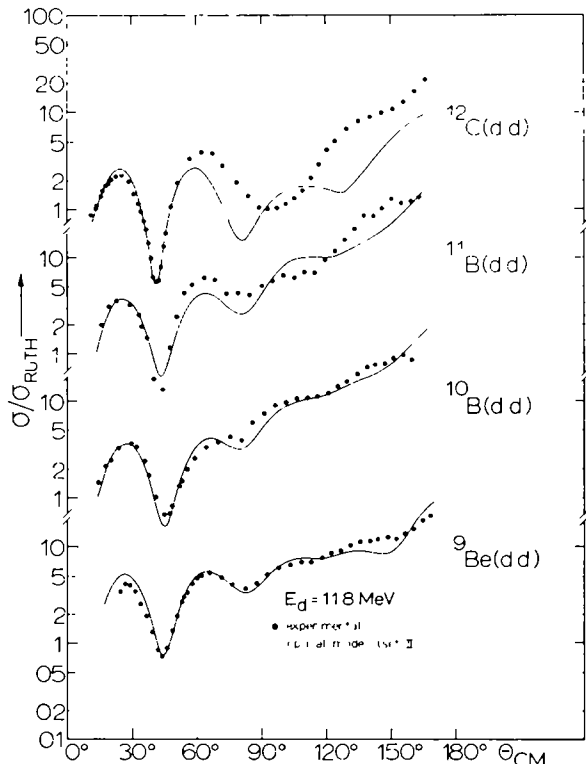


Fig. 2 Experimental angular distributions of the elastic deuteron scattering from Be, ^{10}B , ^{11}B and C. The solid curves give the results of the ABACUS optical-model search with type II parameters.

extended to larger backward and smaller forward angles, respectively, and the measurement of the oxygen absolute cross section has been improved. Fig. 1 shows the measured differential cross sections divided by the Rutherford cross section. The general structure of the curves is very similar. They show a sharp minimum at $\theta_{\text{cm}} = 40 \dots 45^\circ$, and the cross section in backward angles is rather high. On the

other hand, the detailed structure of the angular distributions varies for different nuclei.

Angular distributions of deuterons inelastically scattered from the following levels have been investigated in this work: ${}^9\text{Be}$: $E_x = 2.43$ MeV, ${}^{10}\text{B}$: $E_x = 0.72, 2.15, 3.59, 4.77, 5.11, 5.92 + 6.02 + 6.13$ MeV (the three levels at about 6 MeV excitation energy have not been resolved, the main contribution is known⁵) to come from the 6.02 MeV level, and ${}^{12}\text{C}$: $E_x = 4.43$ MeV. All these distributions are rather smooth (figs. 3 and 4). The differential cross sections of the various levels in the ${}^{10}\text{B}(\text{d}, \text{d}')$ reactions taken at $\theta_{\text{cm}} = 70^\circ$ (i.e. in the minima of the angular distributions) fit surprisingly well to a $(2J+1)$ dependence, where J is the spin of the excited level. An

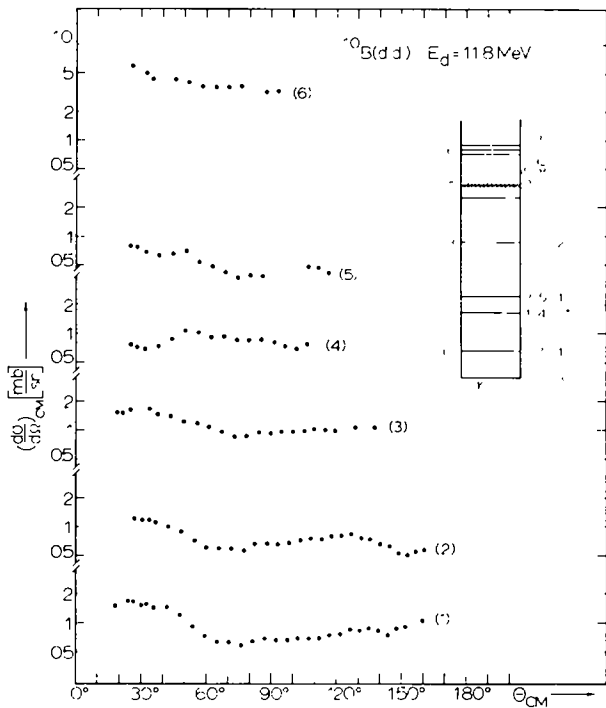


Fig. 3 Experimental angular distributions of the ${}^{10}\text{B}(\text{d}, \text{d}')$ reaction.

excitation of the $T = 1$ levels has not been detected within our experimental accuracy. The results of the (d, t) and $(\text{d}, {}^3\text{He})$ measurements on ${}^{11}\text{B}$ are shown in fig. 5. The absolute cross sections for the reactions on ${}^{10}\text{B}$ and ${}^{11}\text{B}$ were determined within an accuracy of $\pm 25\%$, the major source of error being the target thickness. This error is the same for both isotopes, because elastic scattering data have been taken with one boron target of known isotopic composition. The relative errors are about $\pm 8\%$ for the elastic data and $\pm 14\%$ in the case of the pick-up reactions.

4. Optical-model analysis

The optical model has proved to give a good account of the elastic scattering data on light nuclei, if one energy and one target nucleus are considered only: Difficulties arise in analysing data at different energies or target nuclei with a common set of parameters⁶⁻⁸). The aim of our work was to look for consistent parameters which describe the elastic deuteron scattering on various light target nuclei. The optical potential used was of the form

$$U(r) = V_C(r) - Vf(r) - iWg(r) - V_{s.o.}h(r)(\mathbf{l} \cdot \boldsymbol{\sigma}),$$

$V_C(r)$ is the Coulomb potential resulting from a uniform charge distribution of radius 1.3 fm $A^{\frac{1}{3}}$,

$$\begin{aligned} f(r) &= (1 + e^x)^{-1}, \\ g(r) &= \begin{cases} 4(d/dx')(1 + e^{x'})^{-1} & (\text{type I}), \\ (1 + e^{x'})^{-1} & (\text{type II}), \end{cases} \\ h(r) &= (\hbar/m_\pi c)^2 r^{-1} (d/dr)(1 + e^x)^{-1}, \\ x &= (r - r_0 A^{\frac{1}{3}})/a, \quad x' = (r - r'_0 A^{\frac{1}{3}})/a', \end{aligned}$$

where A is the atomic mass number.

TABLE 1
Optical model parameters for elastic scattering of 11.8 MeV deuterons

Type I

Nucleus	V (MeV)	r_0 (fm)	a (fm)	W (MeV)	r'_0 (fm)	a' (fm)	$V_{s.o.}$ (MeV)
⁹ Be	118.0	0.869	1.01	6.87	1.68	0.879	6.0
¹⁰ B	118.0	0.863	0.916	5.44	1.59	0.716	6.0
¹¹ B	118.0	0.895	0.902	4.82	1.62	0.775	5.8
¹² C	118.0	0.887	0.928	6.11	1.52	0.790	5.0
¹⁴ N	118.0	0.866	0.893	5.59	1.42	0.727	6.0
¹⁶ O	118.0	0.934	0.792	5.95	1.58	0.777	6.0

TABLE 2
Optical model parameters for elastic scattering of 11.8 MeV deuterons

Type II

Nucleus	V (MeV)	r_0 (fm)	a (fm)	W (MeV)	r'_0 (fm)	a' (fm)	$V_{s.o.}$ (MeV)
⁹ Be	78.0	0.967	1.04	30.0	1.07	0.870	6.05
¹⁰ B	78.0	0.921	0.943	30.0	0.867	0.731	6.00
¹¹ B	78.0	0.981	0.989	30.0	0.901	0.759	5.91
¹² C	78.0	1.15	0.930	30.0	1.04	0.864	6.11

The fitting procedure was carried out with the parameter search code ABACUS[†]. Two different types of potentials have been used. Type I is characterized⁶) by a

[†] The authors are indebted to E. H. Auerbach for making this program available to them.

surface absorption term with considerably larger radii for the imaginary than for the real part of the potential, whereas type II has⁹) volume absorption and nearly equal radii for the real and the imaginary part (see tables 1 and 2). Figs. 1 and 2 show the results of our calculations. The type I parameters describe our data fairly well, mainly for the heavier elements, whereas the type II set gives a better account for the Be(d, d) and ¹⁰B(d, d) angular distributions. The type II parameters fail to fit the data on the heavier nuclei accurately. In the final search of type I parameters, all four geometric parameters (r , a , r' and a') and W were allowed to vary. Calculations with fixed r and r' (V , a , W and a' varied) reproduced the experimental data less accurately, particularly for the lightest nuclei. The inclusion of a spin-orbit term turned out to be essential in getting a good fit, although only $(l \cdot \sigma)$ terms for spin $\frac{1}{2}$ could be handled in the search routine used. Spin-1 calculations were performed with the code JULIE[†] and showed only minor differences to the spin- $\frac{1}{2}$ results, using the same depth $V_{s.o.}$. The strength of the spin-orbit term was only poorly determined by the elastic scattering data, since for different values of $V_{s.o.}$ equivalent fits have been obtained by small variations of the imaginary potential. Therefore the final search with the type I parameters was performed with fixed spin-orbit strengths.

5. Inelastic scattering

One may take the smooth angular distributions of (d, d') reactions on light nuclei together with the observed $(2J+1)$ proportionality of the ¹⁰B(d, d') cross sections as an indication for compound nuclear contributions. Calculations with the DWBA

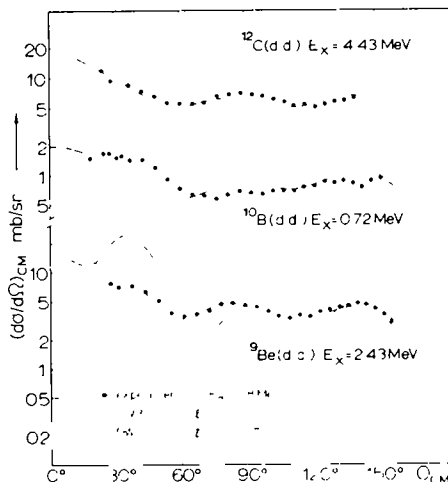


Fig. 4 Experimental angular distributions of the reactions ⁹Be(d, d'), $E_x = 2.43$ MeV, ¹⁰B(d, d') $E_x = 0.72$ MeV and ¹²C(d, d') $E_x = 4.43$ MeV. The solid and dotted lines correspond to DWBA calculations with parameters of type I and type II, respectively. A collective-model form factor was used in complex coupling.

[†] The authors are indebted to R. M. Drisko for making this program available to them.

code JULIE, however, show, that the angular distributions may also be fitted by assuming a single-step collective excitation. (This has been done again only for "spin-½ deuterons".)

A reasonable fit to the data has been obtained from set I parameters (with different radii and surface absorption) using a complex coupling interaction (see fig. 4). Similar calculations using set II parameters as well as real coupling interaction with both sets of parameters failed to fit the data.

6. DWBA analysis of the (d, t) and ($d, {}^3He$) reactions

The angular distributions of the (d, t) reactions on 9Be , ${}^{10}B$ and ${}^{11}B$ and of the ($d, {}^3He$) reactions on ${}^{10}B$ and ${}^{11}B$ are shown in figs. 5–7. All distributions display a typical pick-up pattern suggesting a predominantly direct interaction mechanism. Therefore a DWBA analysis was performed in order to test the deuteron potentials obtained in sect. 4 and to study the applicability of the usual DWBA theory to

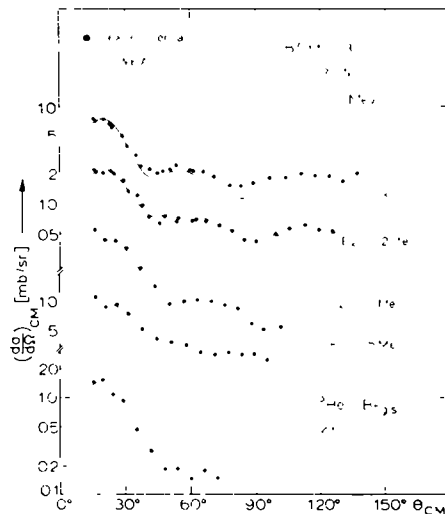


Fig. 5. Experimental angular distributions of tritons and 3He particles from the reactions ${}^{11}B(d, t){}^{10}B$ and ${}^{11}B(d, {}^3He){}^{10}Be$. For details of the DWBA calculations see text.

these light nuclei. Unfortunately no proper optical parameters from elastic scattering were available at the energies of the outgoing particles in the (d, t) and ($d, {}^3He$) reactions considered. However, some published elastic 3He and triton scattering data^{10–12}) could be used which approximately correspond to the exit channel situation in our pick-up measurements. These elastic data have been re-analysed in order to get consistent parameters with real potentials between 130 and 160 MeV. Again the code ABACUS has been used, and the optical potential was of the same form as type I in sect. 4. It turned out that different real potentials depths were necessary

to fit the elastic angular distributions on ${}^9\text{Be}$ and ${}^{12}\text{C}$. Using the Vr^n ambiguity this difference can be transformed to a variation of r_0 which is very similar to the trend observed in the elastic deuteron scattering radii from sect. 4 (tables 1 and 2). Good fits to the ${}^9\text{Be}({}^3\text{He}, {}^3\text{He})$, ${}^{12}\text{C}({}^3\text{He}, {}^3\text{He})$ and ${}^{12}\text{C}(t, t)$ data were obtained in our

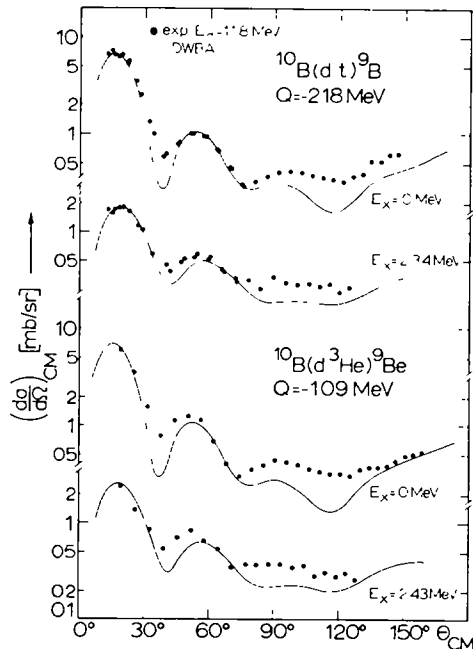


Fig. 6. Experimental angular distributions of tritons and ${}^3\text{He}$ particles from the reactions ${}^{10}\text{B}(d, t){}^9\text{B}$ and ${}^{10}\text{B}(d, {}^3\text{He}){}^9\text{Be}$. The solid curves correspond to DWBA predictions.

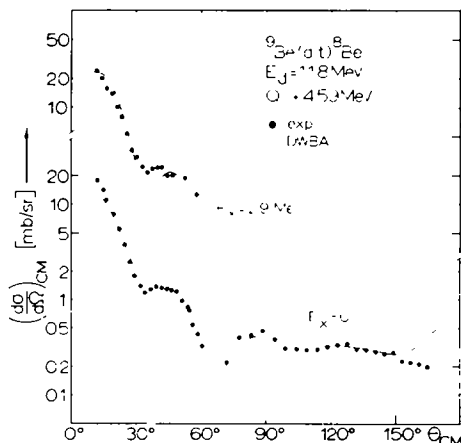


Fig. 7. Experimental angular distributions of tritons from the ${}^9\text{Be}(d, t){}^8\text{Be}$ reaction. The solid curves correspond to DWBA predictions.

optical-model analysis for all energies considered using the parameters shown in table 3. In a recent analysis of elastic ${}^3\text{He}$ scattering on ${}^6\text{Li}$ between 8 and 20 MeV, a similar set of optical parameters has been found¹³⁾.

In the ${}^{11}\text{B}(\text{d}, \text{t})$ reaction, however, where the outgoing particles have very low energies, no satisfactory DWBA fit to all angular distributions could be obtained with one fixed triton potential. Therefore the real well depth of the triton potential was varied in order to optimize the (d, t) fit. Considering only transitions to the $T = 0$ states, a rather well-defined energy dependence of $\delta V/\delta E = 2$ has been found which

TABLE 3
Optical model parameters for the elastic scattering of tritons and ${}^3\text{He}$ -particles

Energy	V_0 (MeV)	r_0 (fm)	r_c (fm)	a (fm)	W (MeV)	r'_0 (fm)	a' (fm)	V_{s0} (MeV)
${}^9\text{Be} + {}^3\text{He}$	6 and 8 MeV	149.3	1.1	1.4	0.733	7.65	1.98	0.7
${}^{12}\text{C} + {}^3\text{He}$	8.5 and 10 MeV	132.3	1.1	1.4	0.756	7.65	1.70	0.7
${}^{12}\text{C} + \text{t}$	12 MeV							5.0

TABLE 4
Spectroscopic factors from our analyses and theoretical predictions from ref. ¹⁴⁾

Reaction	E_x (MeV)	J, T	S_{exp}	S_{theor}
${}^9\text{Be}(\text{d}, \text{t}){}^8\text{Be}$	0	$0^-, 0$	0.51	0.58
	2.9	$2^-, 0$	0.75	0.73
${}^{10}\text{B}(\text{d}, \text{t}){}^9\text{B}$	0	$\frac{1}{2}^-, \frac{1}{2}$	0.80	1.2
	2.34	$\frac{3}{2}^-, \frac{1}{2}$	0.64	0.91
${}^{10}\text{B}(\text{d}, {}^3\text{He}){}^9\text{Be}$	0	$\frac{1}{2}^-, \frac{1}{2}$	0.76	1.2
	2.43	$\frac{3}{2}^-, \frac{1}{2}$	0.66	0.91
${}^{11}\text{B}(\text{d}, \text{t}){}^{10}\text{B}$	0	$3^-, 0$	1.88	1.1
	0.72	$1^+, 0$	0.94	0.26
	1.74	$0^+, 1$	1.35	0.64
	2.15	$1^+, 0$	1.35	0.53
	0	$0^+, 1$	1.28	0.64

was still consistent with the elastic data. A similar trend in the energy dependence was observed in the ${}^{13}\text{C}({}^3\text{He}, {}^3\text{He})$ reaction¹⁴⁾. For the ${}^{11}\text{B}(\text{d}, {}^3\text{He})$ reaction, the "best fit" ${}^3\text{He}$ potential was found to be about 8 MeV deeper than the triton potential of the corresponding energy. This may well be explained by a $(\text{t} \cdot \text{T})$ term in the optical potential¹⁵⁾.

This term is zero in the exit channel of the ${}^{11}\text{B}(\text{d}, \text{t}){}^{10}\text{B}$ ($T = 0$) reaction, whereas the diagonal term $(t_z T_z)U_1$ takes the value $\frac{1}{2}U_1$ in the ${}^{11}\text{B}(\text{d}, {}^3\text{He}){}^{10}\text{Be}$ ($T = 1$) reaction (U_1 is the isospin potential). As stated in ref.¹⁶⁾, the angular distribution of the (d, t) transition to the $T = 1$ state in ${}^{10}\text{B}(E_x = 1.74 \text{ MeV})$ is different from the

angular distributions to the $T = 0$ states and resembles its analogue transition $^{11}\text{B}(\text{d}, ^3\text{He})^{10}\text{Be}_{g+}$. The “best-fit” triton potential to this state turned out to have the same well depth as the ^3He potential for the $^{11}\text{B}(\text{d}, ^3\text{He})^{10}\text{Be}_{g+}$ reaction. However, no simple conclusions on the isospin potential can be drawn from this coincidence, because the $(t_z T_z)$ term is always zero in the (d, t) transitions for $T = 1$ as well as for $T = 0$ final states. Thus isospin-dependent effects can be produced only by off-diagonal terms.

For the entrance channel the two deuteron potential sets of sect. 4 were available, but as in our elastic and inelastic scattering analyses, set I was superior also in the pick-up reactions. Therefore these parameters were used exclusively throughout the analysis. Since in the code JULIE local wave functions and the zero-range approximation are used, non-locality corrections¹⁷⁾ for both the bound state and the scattering wave functions as well as finite-range corrections¹⁸⁾ have been calculated in the local-energy approximation using the program ROMEO. The final DWBA curves including all corrections described are shown in figs. 5–7 together with the experimental results. In cases where p_3 as well as p_4 transitions were allowed from angular momentum conservation, calculations have been performed using as well $j = \frac{1}{2}$ as $j = \frac{3}{2}$. The shapes of the corresponding DWBA curves were found to be not very different. Thus figs. 5–7 show the DWBA fits for the predominant transitions¹⁹⁾ only, i.e. $j = \frac{3}{2}$ in all cases except $^{11}\text{B}(\text{d}, \text{t})^{10}\text{B}$, $E_\chi = 0.72$ MeV with $j = \frac{1}{2}$. The spectroscopic factors, however, have been extracted by the DWBA analyses using the p_3 to p_1 ratios from the calculations of Cohen and Kurath¹⁹⁾.

For the evaluation of absolute spectroscopic factors, the normalization constants of Bassel²⁰⁾ have been used, i.e. 3.3 for (d, t) and 2.95 for $(\text{d}, ^3\text{He})$. The absolute spectroscopic factors extracted by means of these analyses are given in table 4. Within the experimental accuracy and the usual uncertainties in DWBA analyses, the results for the pick-up reaction on ^9Be and ^{10}B agree well with the intermediate coupling calculations of Cohen and Kurath¹⁹⁾. For $^{11}\text{B}(\text{d}, \text{t})$, however, there are larger deviations from the theoretical S -value. This may be connected with difficulties in applying the DWBA theory to reactions with very negative Q -values and very low energies of the outgoing particles ($E_t = 3.4$ –6.2 MeV in our case). In a (d, t) experiment at $E_d = 21.6$ MeV where those difficulties should be smaller, Dehnhard *et al.*²²⁾ have found better agreement of their relative spectroscopic factors with those calculated by Cohen and Kurath¹⁹⁾.

7. Conclusions

The angular distributions of the elastic scattering of 11.8 MeV deuterons from nuclei between Be and O have been analysed in terms of the optical model. Reasonable parameters have been found in this analysis which vary only slowly from one nucleus to the other. Using these parameters for the entrance channel, satisfactory DWBA fits have been obtained to the (d, t) and $(\text{d}, ^3\text{He})$ data on Be and B. The

extracted absolute spectroscopic factors are in the right order of magnitude or, in several cases in quantitative agreement with intermediate coupling calculations.

The authors wish to thank Professor W. Gentner for his interest in this work. We thank Mr. K. Bähr for his assistance in the (d , ^3He) measurements.

References

- 1) R Jahr, K D Muller, W Oswald and U. Schmidt-Rohr, Z. Phys. **161** (1961) 509
- 2) D Groß, Diplomarbeit, Heidelberg (1963) unpublished
- 3) R Jahr and R Santo, Nuclear Physics **67** (1965) 401
- 4) K Bähr, W Fitz, R Jahr and R Santo, Phys. Lett. **21** (1966) 686
- 5) B H Armitage and R. E. Meads, Phys. Lett. **8** (1964) 346
- 6) G R Satchler, Nuclear Physics **85** (1966) 273
- 7) A A Cowley, G Heymann, R L Keizer and M. J. Scott, Nuclear Physics **86** (1966) 363
- 8) P E Hodgson, Adv. Phys. **15** (1966) 329
- 9) V Valković *et al.*, Phys. Rev. **139** (1965) B331
- 10) L. G. Earwaker, Nuclear Physics **A90** (1967) 56
- 11) J J Schwartz, W. P. Alford, L. M. Blau and D Cline, Nuclear Physics **88** (1966) 539
- 12) R N Glover and A D. W. Jones, Phys. Lett. **16** (1965) 69
- 13) H Ludecke, Tan Wan-Tjin, H Werner and J Zimmerer, MPI Heidelberg, Jahresbericht (1966) and to be published
- 14) L M Kellogg and R W. Zurmuhle, Phys. Rev. **152** (1966) 890
- 15) A M Lane, Nuclear Physics **35** (1962) 676
- 16) H Fuchs and R Santo, Phys. Lett. **24B** (1967) 234
- 17) F G Percy and D. Saxon, Phys. Lett. **10** (1964) 107
- 18) J K Dickens, R. M Drisko, G F Percy and G R Satchler, Phys. Lett. **15** (1965) 337
- 19) S Cohen and D Kurath, Nuclear Physics **73** (1965) 1
- 20) R H Bassel, Phys. Rev. **149** (1966) 791
- 21) D. Dehnhard, G C. Morrison and Z Vager, Int Conf nuclear physics session 1-29, Gatlinburg (1966)